Molybdenum sputtering film characterization for high gradient accelerating structures

S. Bini[1] B. Spataro[1;1)] A. Marcelli[1,2;2)] S. Sarti[3] V. A. Dolgashev[4] S. Tantawi[4]
A. D. Yeremian[4] Y. Higashi[5] M. G. Grimaldi[6] L. Romano[6] F. Ruffino[6]
R. Parodi[7] G. Cibin[8] C. Marrelli[9] M. Migliorati[9] C. Caliendo[10]

[1] INFN - LNF, Via E. Fermi 40, Frascati (RM) 00044, Italy
[2] NSRL, University of Science and Technology of China, Chinese Academy of Sciences, Hefei 230029, China
[3] University of Rome - Sapienza, Dipartimento di Fisica, Piazzale Aldo Moro 5, Rome 00185, Italy
[4] SLAC National Accelerator Laboratory, 2575 Sand Hill Road, Menlo Park, CA 94025, USA
[5] KEK 1-1 Oho, Tsukuba, Ibaraki 305, Japan
[6] University of Catania, Dipartimento di Fisica e Astronomia & MATIS-IMM-CNR, Via S. Sofia 64, Catania 95123, Italy
[7] INFN-Genova, Via Dodecaneso 33, Genova 16146, Italy
[8] Diamond Light Source, Chilton, Didcot, Oxford OX110DE, UK
[9] University of Roma - Sapienza, Dipartimento di Scienze di Base e Applicate per l'Ingegneria, Via A. Scarpa, Roma 14 - 00161 - Italy
[10] Istituto dei Sistemi Complessi, ISC-CNR, Area della Ricerca di Roma 1, Via Salaria km 29.300, Monterotondo, Rome 00040, Italy

Abstract: Technological advancements are strongly required to fulfill the demands of new accelerator devices with the highest accelerating gradients and operation reliability for the future colliders. To this purpose an extensive R&D regarding molybdenum coatings on copper is in progress. In this contribution we describe chemical composition, deposition quality and resistivity properties of different molybdenum coatings obtained via sputtering. The deposited films are thick metallic disorder layers with different resistivity values above and below the molibdenum dioxide reference value. Chemical and electrical properties of these sputtered coatings have been characterized by Rutherford backscattering, XANES and photoemission spectroscopy. We will also consider multiple cells standing wave section coated by a molybdenum layer designed to improve the performance of X-Band accelerating systems.

Key words: linear accelerator, cavities, X-band, coatings, XANES, resistivity

PACS: 29.20.Ej, 68.55.-a, 61.05.cj **DOI:** 10.1088/1674-1137/37/9/097005

1 Introduction

The next generation of linear accelerators is highly demanding in terms of accelerating gradients. Indeed, the accelerating gradient is one of the major parameters of a linear accelerator since it determines the accelerator length and its power consumption. Although the accelerating gradient of normal conducting accelerating structures is mainly limited by the RF breakdown, the experience shows that obtaining high gradients with a normal-conducting structure requires operation at a relatively high frequency. To minimize costs, the availability of advanced high frequency accelerating structures is one of the main goals of the accelerators community. To upgrade performances of the X band Linacs at 11.424 GHz, resources and efforts are then devoted to achieve the highest accelerating gradients and at the same time the highest possible reliability. In the framework of a large collaboration among SLAC (Stanford Linear Accelerator Center), KEK (Kō Enerugī Kasokuki Kenkyū Kikō) and the INFN-LNF laboratory, efforts are devoted to design, manufacture and test short high power standing wave (SW) sections.

Among the many, manufacture technologies and surface properties are fundamental issues of advanced cavities. Electroplating is a very attractive technique to manufacture compact structures avoiding the soft brazing while maintaining mechanical properties and high-vacuum requirements. Niobium film technology is also a well-established technology providing considerable benefits over bulk niobium. The reliable performance of niobium thin film cavities allows their use at LEP [1] and LHC [2] although it is not clear if this technology should be used for new accelerators such as ILC ([1] and

Received 28 October 2012, Revised 12 March 2013
1) E-mail: bruno.spataro@lnf.infn.it
2) E-mail: marcelli@lnf.infn.it

therein). Molybdenum is an interesting material for accelerator components and a stimulating option for RF linear accelerating structure characterized by low breakdowns at high RF power. For application in high gradient accelerating structures, data of Mo breakdown rate and its electric field are already very promising if compared with Cu materials [3]. A brazed molybdenum bulk X-band RF structure has also recently been manufactured and tested at high power at SLAC. This brazed Mo structure with the same RF parameters exhibited a breakdown rate higher than a similar copper structure. However, a drawback of the manufacturing of sintered molybdenum bulk is the long time required to machine the cavity, a 300 nm surface roughness using "tungsten carbide" tools, the gas contamination and an uneven loading stress in the brazed region. Additionally, technological problems have also been detected in sintered molybdenum bulk brazed sections [4, 5]. To overcome drawbacks associated with the use of sintered molybdenum bulk [6], we started a feasibility study with a single sputtering technique to make copper cavity resonators characterized by a low surface roughness and then to deposit a molybdenum film on top in order to reduce the breakdown phenomenon. A molybdenum sputtering method has been tested as a possible route to achieve accelerating electric field performance of normal conducting structures operating at 11.424 GHz. This research will certainly be useful to improve properties of normal conducting devices and the related manufacture technologies. Although, as will be described later, setting of Mo deposition parameters is not the main issue, a lot of work is necessary to fully characterize these devices and, in particular, their conductivity properties and behavior under high fields, because future dedicated RF cavities have to be manufactured and tested at higher power [7]. We present here a characterization of high-quality Mo coatings on Cu, their chemical composition and resistivity measurements with the final goal to design and manufacture an SW structure made of copper cells coated with Mo.

2 Molibdenum coatings on copper

We performed this study at the Laboratori Nazionali di Frascati of the INFN where we recently set up facilities for surface coating treatments. We used copper samples of 2 cm diameter, 3 mm thick on top of which we deposited a molybdenum film. The method is based on a magnetron sputtering configuration. Studies have shown that molybdenum thin films are easily deposited by RF magnetron sputtering (a less sensitive technique), achieve a good adhesion to the substrate and, with the same conditions of argon pressure and RF power, are characterized by a better surface quality than similar coatings deposited by the DC magnetron sputtering method. Also the grain sizes of the deposited films grow with similar parameters. A DC glow discharge procedure has been adopted before each treatment in order to clean the inner surfaces of the vacuum chamber and remove water from the environment. The glow discharge was stabilized at 1.5 A resulting in a potential of ∼200 V between the central molybdenum anode and the grounded vacuum chamber. The RF sputtering discharge was established in a noble gas atmosphere (argon for standard coatings) in the pressure range of $1\div15\times10^{-3}$ mbar. The coating took place at room temperature and a thickness of about 0.7 μm was typically obtained after 25 minutes. The distance between samples and the molybdenum target is about 8 cm at the magnetic induction of about 100 G. To evaluate the surface quality and to understand the morphological aspects we used an atomic force microscopy (AFM). In Fig. 1 we show one surface of the machined copper with a roughness of ∼70 nm before the molybdenum sputtering process. Clear undulations of the surface due to the step of the lathe machine (∼700 nm) with many overlapping spikes appear.

In Fig. 2 the same spikes disappear after a deposition of a Mo layer of ∼100 nm molybdenum. The film on the

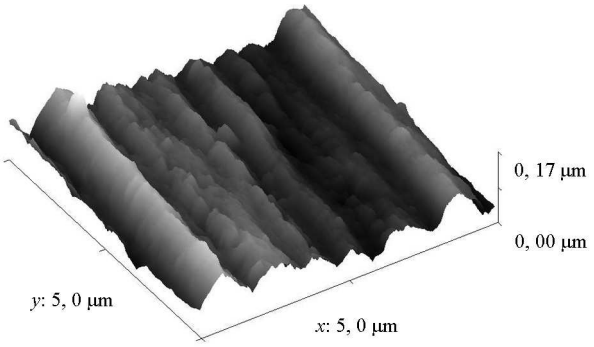

Fig. 1. AFM image of the surface of a copper sample before the molybdenum sputtering.

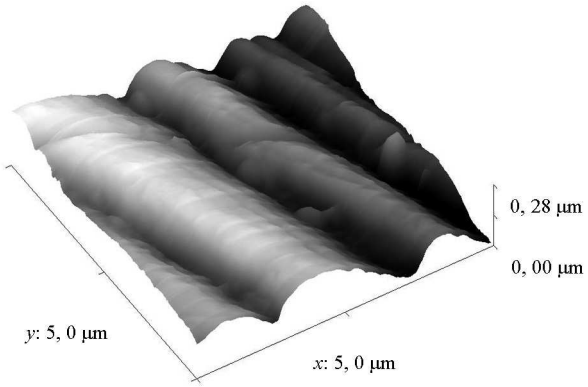

Fig. 2. AFM image of deposited molybdenum on copper by the sputtering technique.

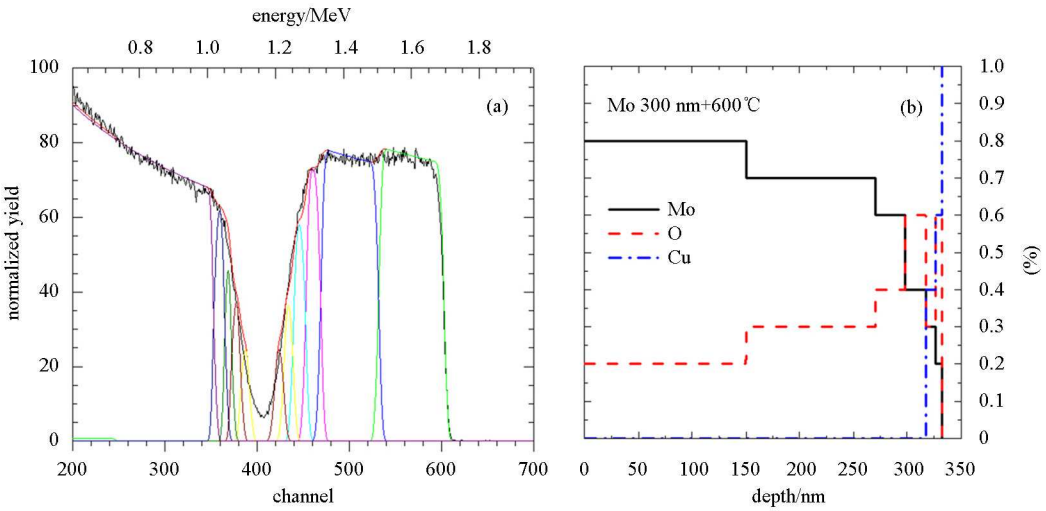

Fig. 3. (color online) (a) 2 MeV He RBS spectrum of Mo film deposited on Cu (black line). The RUMP simulation of the whole sample (red line) has been obtained with different layers (colored lines) containing Mo, O and Cu; (b) The resulting profiles of Mo, O and Cu as a function of depth.

copper surface acts like a smooth layer improving the roughness of the surface. Actually, our tests confirm that the initial low roughness of the Cu machined surface is preserved or improved by Mo sputtering. However, since Cu and Mo have different thermal coefficients, the molybdenum deposited layer on top of copper is not stable vs. temperature. After deposition, to stabilize the Mo coating we performed a dedicated thermal treatment to fix the film on the substrate [3]. The procedure allowed achievement of homogeneous coatings and a reasonable contact force between the Mo layer on top of the copper.

To obtain information regarding the chemical composition of the coating as a function of the depth profile of the deposited molybdenum we used the Rutherford backscattering spectroscopy (RBS) [3]. As an example, the depth profile analysis of a 350 nm molybdenum film is shown in Fig. 3 as obtained after a thermal treatment at 600 C for 2 hours. The curve shows the atomic concentration of the relevant components of the deposited film vs. the distance from the sample surface. Data indicate that the film is uniformly contaminated vs. depth by oxygen (∼20%). Similar results have been obtained by photoemission spectroscopy data [3].

3 XAS (X-ray Absorption Spectroscopy) characterization

To characterize the chemical status of Mo atoms we performed XAS (X-ray Absorption Spectroscopy) experiments at the Mo K edge, moreover, working at grazing incidence we may enhance the signal associated to thin surface layers. X-ray Absorption Spectroscopy is a well-established technique that via methods such as EXAFS (Extended X-Ray Absorption Fine Structures) or XANES (X-ray Absorption Near Edge Structure) may return a direct quantitative measurement of local structure properties such as geometry, bond lengths and coordination numbers around a selected photo-absorber also in non-crystalline and amorphous systems [8]. With EXAFS we are also able to recognize the nature of the nearest neighbors around a photo-absorber atom while using XANES spectroscopy, a technique that looks at the intense features present in a short energy range around the atomic edge, we may obtain geometrical information of a small cluster around the photoabsorber. It has been well demonstrated that using XAS spectroscopy, a series of spectral characteristics, e.g., the position of the absorption threshold, depend on the electronic properties of the photoabsorber (in our case Mo) and therefore on its state of oxidation. The shape of the spectrum is characteristic of an atomic coordination, e.g., tetrahedral or octahedral, and also the presence of pre-edge structures may clarify coordination and oxidation of a photo-absorber.

Experiments at the Mo K-edge have been performed at Diamond on the beamline B18 using a Si(111) monochromator coupled to a Pt coated mirror focusing radiation in a spot of ∼200×200 μm [9]. Fluorescence radiation has been measured by a 9-elements Ge detector and a readout electronics XSPRESS2 collecting ∼300 kcs/sec per element. The incoming radiation has been monitored using an ionization chamber filled by Ar gas.

To optimize signals from Mo atoms, experiments have been performed both at grazing incidence and at normal incidence in different areas of the film always in the fluorescence mode. As an example, in Fig. 4 we show XANES data at the Mo K-edge of a Mo coated film (∼600 nm) on a Cu disk of ∼2 cm of diameter.

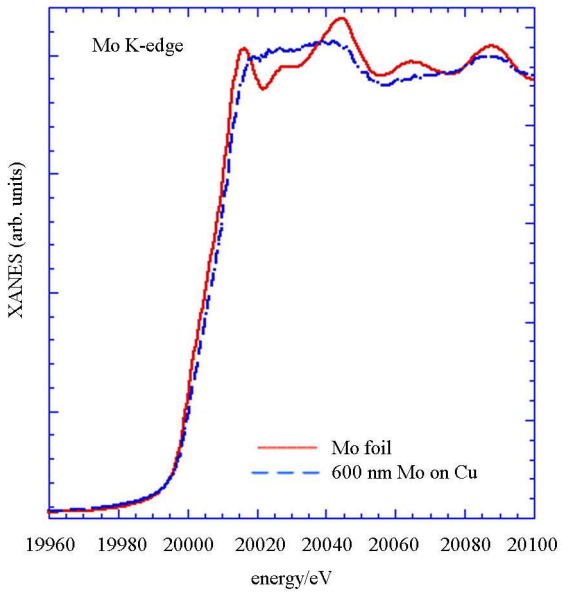

Fig. 4. (color online) Comparison of spectra at the Mo K-edge between a Mo film (red) and a Mo coating on a copper disk (blue).

From these data, analyzing the shift of the energy position of the absorption threshold it is possible to identify the oxidation state of Mo. Looking at Fig. 4 the comparison of XANES spectra between a Mo film measured in the transmission geometry and a 600 nm Mo coated layer on a copper disk measured at grazing incidence, we may point out that the Mo coating has a slightly disordered structure (see the smoothed features at the edge). Moreover, from the comparison with the available XANES spectra of different Mo oxides [6] we may also recognize that these coatings are made by Mo dioxide (MoO_2) i.e., a Mo atom coordinated by four oxygen atoms. The result is confirmed by the observed shift of the absorption edge (∼3 eV) in agreement with Mo dioxide XAS data available in the literature [10].

4 Electrical characterization

The electrical properties of Mo sputtered coatings have been measured via sample surface impedance probed as a function of the frequency through a Corbino disk geometry. In the latter the sample shortcircuits the coaxial cable connecting the sample to the instrument: a Vector Network Analyzer Anritsu 37297D. The connection between the cable and the sample was made through a double spring method, extensively described in Ref. [11] (see Fig. 5). The measured quantity is the microwave reflection coefficient, that is the complex ratio between the reflected wave and the incident one, measured at the instrument port. This coefficient can be related through standard line calibration to the reflection coefficient at the interface between the connector and the sample under measurement. Indeed, the calibration process is possible only down to the plane which separates the coaxial cable from the connector depicted in the figure. The very last section of the line, that is the connector, cannot be fully calibrated, and a different approach has to be used. The connector used is a commercial V103F (Anritzu) launcher, whose inner and outer diameters are 0.7 and 1.4 mm respectively. Comparing these numbers to the lateral dimensions of the samples, it is evident that only a rather small section of the sample is probed. For this reason, we may approximate the sample as an infinite layer extended in the directions perpendicular to the cable.

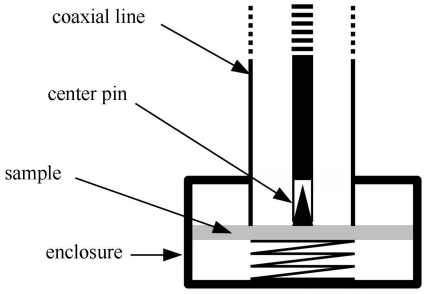

Fig. 5. Sketch of the contact between sample and coaxial line.

4.1 Mode matching (MM) analysis

It is possible to demonstrate that quite generally the reflection coefficient at the interface between the connector and the sample can be written as

$$\Gamma=\frac{Y_0-Y_{\rm eff}}{Y_0+Y_{\rm eff}}, \tag{1}$$

where Y_0 is the line admittance and $Y_{\rm eff}$ is an effective admittance of the sample, which depends on the resistivity as well as on the geometry of the sample. The expression of $Y_{\rm eff}$ is in general quite complex (especially at high frequencies). For the special case of a sample infinitely extended in the directions perpendicular to the wave propagation (the so-called "open ended" geometry), the effective admittance has been calculated by Ganchev et al. [12]. Their result can be written in the following form:

$$Y_{\rm eff}=\int_0^\infty K(\zeta,k_0)Y_{\rm s}(\zeta){\rm d}\zeta, \tag{2}$$

where $K(\zeta,k_0)=k_0 s_{\rm ab}(k_0\zeta)$ with $s_{\rm ab}(x)=[J_0(xb)-J_0(xa)]^2/(x\ln(b/a))$, J_0 is the Bessel function and a e b are the inner and outer radius of the coaxial cable, while $Y(\zeta)=\omega\tilde{\epsilon}/k(\zeta)$, with $k(\zeta)=k_0\sqrt{\tilde{\epsilon}_{\rm r}-\zeta^2}$. In these expressions $k_0=\omega/c$ (with c the speed of light in vacuum and $\omega=2\pi\nu$) and $\tilde{\epsilon}$ is the (relative) complex permittivity of the material under study which, for a solid material at microwave frequencies is usually written as

$$\tilde{\epsilon}=\epsilon_{\rm r}-{\rm i}\frac{1}{\epsilon_0\rho\omega}, \tag{3}$$

where ϵ_r is the relative dielectric constant and ρ the dc resistivity[1)]. If the sample is a relatively thin film grown on a substrate, the expression for the effective admittance must take into account also further reflections that occur at the "end" of the sample, that is at the interface between the film and the substrate. In the "open ended" geometry [12] the expression for the effective admittance changes to

$$Y_{\rm eff}=\int_0^\infty K(\zeta,k_0)\left\{Y_{\rm s}(\zeta)\frac{\bar{Y}_{\rm b}(\zeta)+{\rm i}Y_{\rm s}(\zeta)\tan[k_{\rm s}(\zeta)d_{\rm s}]}{Y_{\rm s}(\zeta)+{\rm i}\bar{Y}_{\rm b}(\zeta)\tan[k_{\rm s}(\zeta)d_{\rm s}]}\right\}{\rm d}\zeta, \tag{4}$$

where the subscript "s" refers to parameters of the sample and the subscript "b" refers to parameters of the "backplate", that is, the substrate. $\bar{Y}_{\rm b}(\zeta)$ is the effective admittance of the substrate, which has an expression analogous to the expression within parentheses in equation 4 (in the special case of an infinitely thick substrate, $\bar{Y}_{\rm b}(\zeta)=\omega\epsilon_{\rm b}/k_{\rm b}(\zeta)$).

4.2 Calibration of the line

Although a full calibration of the last section of the line (that is the connector) is not possible, a partial calibration can be made by using three "known" samples. In fact, we recall that quite generally the reflection coefficients measured on two different planes of a microwave line are related to each other by the relation

$$\Gamma_1(\nu)=E_{\rm d}(\nu)+\frac{E_{\rm r}(\nu)\Gamma_2(\nu)}{1-E_{\rm s}(\nu)\Gamma_2(\nu)}, \tag{5}$$

where $E_{\rm r}$, $E_{\rm s}$ and $E_{\rm d}$ are frequency dependent, complex coefficients related to the properties of the segment of the line between the two sections 1 and 2. In particular, $E_{\rm r}$ accounts for the attenuation and phase shift of the microwave during the travel across the line segment, $E_{\rm s}$ and $E_{\rm d}$ take into account possible reflections of the microwave signal within the line segment. Since none of the three coefficients are known a priori, a full calibration would require the measurement of three curves $\Gamma_1(\nu)$ and the calculation of three curves $\Gamma_2(\nu)$. Two of these curves can be obtained by measuring a polished copper plate (which is a good approximation of an infinitely conductive sample) and the glass side of one of the Mo/glass samples (whose calculated corresponding curve depends almost only on the glass parameters). For the third curve, we use one of the Mo samples grown on a glass substrate, whose thickness and dc resistivity have been measured independently.

This procedure would provide a full calibration of the line if it were possible to measure these samples with very high precision and to exactly know the parameters defining the electric response of the three measured samples. However, due to the non-perfect contact between the connector and the measured sample, the measurement cannot be as precise as it would be requested by a calibration procedure. Moreover, the parameters describing the samples are known only to a relatively low precision, introducing a further source of possible error. As a result, this calibration cannot be as precise as the calibration of the remaining part of the line, where connections between line segments are realized through high precision connectors.

The results of this procedure are the curves represented with open dots in Fig. 6. Data point out that oscillations are due to the connector and after calibration reliable resistivity values can be obtained.

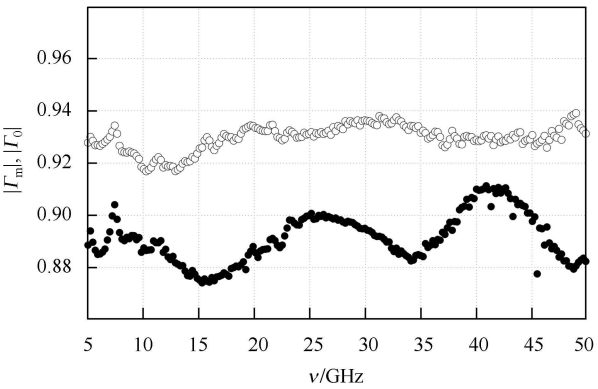

Fig. 6. Measurements on the Mo film grown on glass substrate (see below). Filled symbols are raw data, open symbols the reflection coefficient at the film surface as obtained through the calibration procedure described in the text.

4.3 Results

In our coated films, although a priori we cannot exclude the presence of a thin oxide layer between the sample and the substrate we clearly have a Mo-based film grown on a copper substrate [10]. In this case a detailed measurement of the Mo resistivity is extremely difficult. In fact, it can be easily shown that, due to the thickness of the Mo film, $\tan(k_{\rm s}(\zeta)d_{\rm s})\ll 1$ so that, since further $Y_{\rm s}<Y_{\rm b}$, equation 4 can be approximated by

$$Y_{\rm eff}\approx\int_0^\infty K(\zeta,k_0)\frac{\bar{Y}_{\rm b}(\zeta)}{1+{\rm i}(\bar{Y}_{\rm b}(\zeta)/Y_{\rm s}(\zeta))\tan(k_{\rm s}(\zeta)d_{\rm s})}{\rm d}\zeta, \tag{6}$$

which, neglecting very special cases, is of the same order of magnitude of $Y_{\rm Cu}=\int_0^\infty K(\zeta,k_0)\bar{Y}_{\rm b}(\zeta){\rm d}\zeta$. Since the latter is much larger than the vacuum admittance Y_0, inserting this result in the equation 7 leads immediately

1) due to the term $\epsilon_0=8.85\times10^{-12}$. Except in very specific cases, it is evident that even in a moderately conducting material the second term largely dominates the first

to the conclusion that for such a sample one always has $\Gamma \approx -1$ for any value of resistivity of the Mo film[1)].

This result is confirmed by measurements on thin Mo films grown on Cu substrate: as can be seen in Fig. 7, the modulus of the uncalibrated reflection coefficient is very close to one, while the behavior of the phase as a function of frequency is due to the short uncalibrated section of the line.

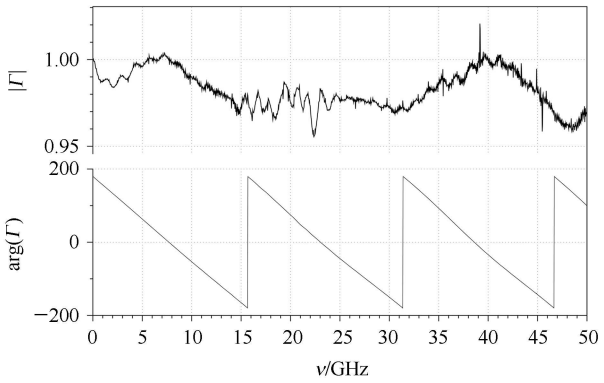

Fig. 7. Modulus (upper panel) and phase (lower panel) of the uncalibrated reflection coefficient for a Mo thin film grown on Cu substrate.

In order to estimate the microwave resistivity of the Mo film, we have performed experiments on Mo films (3000, 6000 and 9000 Å thick) grown on Corning glass and (0001)-oriented single crystal Al_2O_3 substrates, starting from a 4 inch Mo target (99.99%) in Ar (99.9999) atmosphere. The substrates were cleaned with proper solvents in an ultrasonic bath, then they were dried with nitrogen flux. A 30 minute pre-sputtering operation was performed before starting the Mo deposition. The substrate/target distance was 8 cm and the sputtering parameters were the following: background vacuum 4×10^{-7} Torr, rf power 60 W, ambient temperature, pressure during the deposition 4 mTorr, Ar 23 sccm. A calibration curve of film thickness vs. sputtering time at fixed rf power, has been evaluated measuring the film thickness through the optical transmission spectrum. A deposition rate of 300 Å/min was adopted. The films were highly adhesive to the substrates as confirmed by a rudimentary tape test.

The values of resistivity obtained for the samples under study are reported in Table 1 and in Fig. 8. Errors are estimated from the residual behavior as a function of frequency mainly due to the non perfect calibration of the line (Fig. 7, open symbols). These values are compared to the literature values of the resistivity of pure Mo (0.005 mΩ·cm) and of the Mo oxide (0.088 mΩ·cm) in Fig. 8. Similar values are available in the literature [13].

Table 1. Resistivities of the measured samples.

substrate	O_2 pressure	thickness/ nm	ρ/ (mΩ·cm)	$\Delta\rho$/ (mΩ·cm)
glass	10^{-2}	300	1.4	0.1
glass	10^{-2}	600	0.59	0.05
glass	10^{-2}	900	0.49	0.05
glass	1.5×10^{-2}	300	0.07	0.01
glass	1.5×10^{-2}	600	0.12	0.01
glass	1.5×10^{-2}	900	0.10	0.02
glass	10^{-3}	300	0.07	0.01
glass	10^{-3}	600	0.12	0.01
glass	10^{-3}	900	0.13	0.03
Al_2O_3	10^{-3}	300	0.057	0.003
Al_2O_3	10^{-3}	600	0.10	0.006
Al_2O_3	10^{-3}	900	0.08	0.02

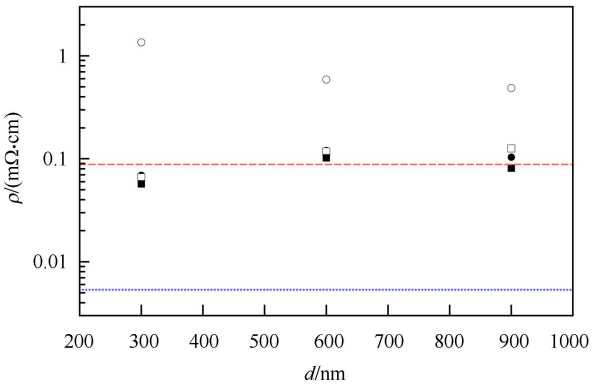

Fig. 8. (color online) Values of resistivity measured on our samples. The resistivity of the first set of samples (open circles), where the presence of MoO_2 has been revealed through RBS and XANES, is sensibly higher than the resistivity of other sets. Also shown, for comparison, the literature values of resistivity for MoO_2 (red dashed line) and pure Mo (blue solid line).

It is clearly evident that the resistivity of samples belonging to the first series are much higher than those of the following series. Comparison with literature data of Mo and MoO_2 points out different contributions of molibdenum oxides that have to be characterized. Work is in progress to understand the differences and associate them with the coating procedures. There are many different types of molybdenum oxides with a different conductivity (see Ref. [6]). The resistivity values we measured are always larger than the literature values for corresponding bulk materials. This is certainly due to the different substrates, the amount of oxygen and the local structures as confirmed by XAS data.

1) This result, derived here for thin Mo films, can be shown to be general: indeed, if the film is very thick ($k_s d_s \gg 1$ or, equivalently, $d_s \gg \delta$), equation 2 holds and, again, the effective admittance of the film is found to be much higher than Y_0

Comparison with literature data of Mo reveals however that in all cases the measured resistivity is much larger than the pure Mo. This is reasonably due to the fact that the structural characterization of the film reveals a relatively high degree of disorder and a non zero amount of oxygen.

With these values it is possible to estimate the ratio between the electric field at the glass surface and the incident field. This is done by calculating the attenuation through the Mo film, which is given by $\exp(-kd)$, with $k = k_0/\sqrt{(4\pi\epsilon_0\nu\rho)}$. This quantity is reported in Fig. 9 for all samples at ν=10 GHz.

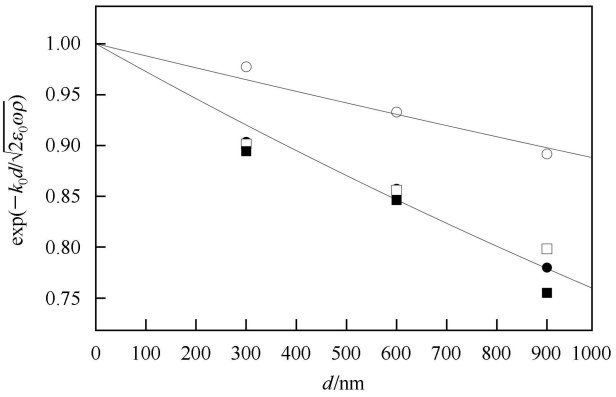

Fig. 9. Ratio between the field at the substrate (glass) surface and the incident field at 10 GHz. The line represents the best exponential fit for the variation as a function of d, for samples belonging to the first series and for all other samples.

As can be easily seen in the figure, the field that reaches the substrate decreases as the thickness of the film increases. In addition, the lower resistivity observed for samples of series 2 to 4 results in a rather large decrease of the "residual" field. Extrapolating the observed attenuation to sample thicknesses of order 1 μm, an attenuation as high as 25% of the electric field (which corresponds to more than 40% of power) can be obtained before the substrate is reached.

4.4 Conclusion

A large effort among INFN-LNF, KEK and SLAC laboratories to characterize and optimize Mo films deposited on Cu is in progress. We point out that molybdenum coatings obtained via sputtering is a promising approach to increase the accelerating gradient of accelerator cavities working at higher frequencies. In this contribution we describe chemical composition, deposition quality and resistivity properties of different molybdenum coatings on copper obtained via sputtering and stabilized by a dedicated thermal treatment. Chemical and electrical properties of these sputtered coatings have been determined by Rutherford backscattering, XANES and photoemission spectroscopies. However, a lot of work still has to be done to improve the quality and performances. Moreover, a full characterization and, in particular, conductivity properties and the behavior under high fields are still in progress because dedicated RF devices with such coatings have to be manufactured and tested at higher power. To optimize performances via coatings of these copper structures, deposition of other materials and different manufacturing methods and characterization of the Mo coatings are in progress. Moreover a SW structure made of copper cells, coated with Mo has been manufactured and it is ready for tests.

We thank Paolo Chimenti for his valuable support to the experimental tests. We also thank Diamond Light Source for the access to the beamline B18 (proposal nt1984-1).

References

1 Gustafsson A et al. New Methods for Thin Film Deposition and First Investigations of The Use of High Temperature Superconductors for Thin Film Cavities. Proceedings of IPAC 2010. Kyoto: Japan, 2010. 2995–2997
2 Descoeudres A, Ramsvik T, Calatroni S et al. PRST- Accelerators and Beams, 2009, **12**: 032001
3 Bini S et al. Development of X-Band Accelerating Structures for High Gradients, RF-11/004, 30/05/11
4 Spataro B, Alesini D, Chimenti V et al. Nucl. Instrum. Methods., 2011, **657**: 114–121
5 Higashi Y, Higo T, Matsumoto S et al. Nucl. Instrum. Methods., 2011, **657**: 156–159
6 Ressler T et al. J. Catal., 2002, **210**: 67–83
7 Bini S, Chimenti V, Marcelli A et al. Chin. Phys. B, 2012, **36**: 639–647
8 Bianconi A, Garcia J, Marcelli A et al. J. Phys. Coll. C9, 1985, **46**: 101–106
9 Dent A J, Cibin G, Ramos S et al. J. Phys. Conf. Ser., 2009, **190**: 012039
10 Cramer S P et al. J. Am. Chem. Soc., 1978, **100**: 3398–3407
11 Tosoratti N et al. Int. J. Mod. Phys. B, 2000, **14**: 2926–2931. Note that using the notation of that paper $Z_0 = 1/Y_0$
12 Ganchev S et al. IEEE Trans. Instrum. Meas., 1995, **44**: 1023–1029
13 Martinez M A, Guillen C. Surf. Coat. Tech., 1998, **110**: 62–67